0026-895X/93/010142-11$03.00/0

MOLECULAR PHARMACOLOGY, 44:142-152

Reconstitution of Glutamate Receptor Proteins Purified from *Xenopus* Central Nervous System into Artificial Bilayers

CATHRYN J. KERRY, HIRA L. SUDAN, KETEVAN ABUTIDZE, IAN R. MELLOR, ERIC A. BARNARD, and PETER N. R. USHERWOOD

Department of Life Science, University of Nottingham, Nottingham, NG7 2RD, UK (C.J.K., H.L.S., I.R.M., P.N.R.U.), and MRC Molecular Neurobiology Unit, Medical Research Council Centre, Cambridge, CB2 2QH, UK (K.A., E.A.B.)

Received August 6, 1992; Accepted April 15, 1993

SUMMARY

Excitatory amino acid (EAA) receptor (EAAR) proteins purified from *Xenopus* central nervous system using a domoate affinity column and then separated into fractions using sucrose density gradient centrifugation were reconstituted, first into liposomes and then into planar lipid bilayers, using pipette-dipping and black lipid membrane techniques. Although the protein was eluted from the column with either α-amino-3-hydroxy-5-methyl-4-isoxazolepropionate (AMPA) or kainate and could not be eluted with *N*-methyl-D-aspartate (NMDA), channel openings were obtained after exposure of the bilayers to kainate, AMPA, or NMDA (usually only in the presence of glycine). In bilayers exhibiting a single open channel conductance level this was ~6 pS with AMPA, ~9 pS with kainate, and ~50 pS with NMDA. However, with a few batches of protein unitary channel openings of up to 400 pS were observed, suggesting that reconstituted EAAR may sometimes form functional aggregates. The protein eluted from the domoate column was divided into two fractions on a sucrose density gradient. After reconstitution, one fraction responded to all three EAAs, whereas the other responded only to the non-NMDA receptor agonists. An explanation for these results is that some of the EAAR eluted from the column contain NMDA receptor subunits in addition to non-NMDA receptor subunits.

L-Glutamate is a major excitatory neurotransmitter in vertebrate CNS, where it activates the EAAR. Pharmacological studies have identified the existence of two classes of EAAR, ionotropic and metabotropic. The ionotropic EAAR gate non-specific, cation-selective, ion channels, whereas the metabotropic receptors function by intracellular signaling through guanine nucleotide-binding proteins (1). There are three subtypes of ionotropic EAAR, NMDAR, AMPAR, and KAINR (1, 2). NMDAR are distinguished from non-NMDAR by their antagonism by phencyclidine and MK-801 (3) and their sensitivity to channel block by Mg^{2+} (4, 5) and Zn^{2+} (6). Responses of NMDAR are potentiated by glycine (4).

There is substantial electrophysiological and biochemical evidence to favor the existence, at least in some parts of vertebrate CNS, of unitary non-NMDAR exhibiting sensitivity to both AMPA and kainate (7). The cloning of cDNAs coding for ionotropic EAAR (8, 9) has revealed many different non-NMDAR subunits (8–15), including a subunit that is insensitive to AMPA (15). Hetero-oligomeric receptors formed from these subunits have been expressed exogenously and shown to exhibit characteristic electrophysiological properties (10, 13, 16), but it remains to be established whether such molecular diversity exists *in vivo*. In this investigation we report on the reconstitution into lipid bilayers of two types of functional EAAR proteins purified from *Xenopus* CNS (a particularly rich source of KAINR) (17, 18). Part of this work has been reported briefly by Henley *et al.* (19).

Materials and Methods

Solubilization of the *Xenopus* brain membranes using the detergent octylglucoside was undertaken as described previously (20), and the EAAR present were purified by affinity chromatography using immobilized domoic acid (or kainate or AMPA) (19). Domoic acid, an analogue of kainate, possesses the highest known affinity for KAINR (21), and >97% of the binding sites for both kainate and AMPA present in the solubilized material were retained by the domoate resin. It was possible to recover equal yields of kainate and AMPA binding sites, as well as a set of binding sites typical of NMDAR, by specific elution from the domoate resin column with either kainate or AMPA.

Two fractions (hereafter called fraction I and fraction II) were obtained from the purified protein (hereafter called total protein) after its concentration in an Amicon (PM10) cell and centrifugation on a 7–15% sucrose density gradient in 0.8% octylglycoside. Fraction I did not exhibit any NMDAR pharmacology in binding studies; fraction II

The research reported herein was sponsored in part by the United States Army, through its European Research Office.

ABBREVIATIONS: CNS, central nervous system; EAAR, excitatory amino acid receptor(s); NMDAR, *N*-methyl-D-aspartate-sensitive receptor(s); KAINR, kainate-sensitive receptor(s); AMPAR, α-amino-3-hydroxy-5-methyl-4-isoxazolepropionate-sensitive receptor(s); EAA, excitatory amino acid; NMDA, *N*-methyl-D-aspartate; AMPA, α-amino-3-hydroxy-5-methyl-4-isoxazolepropionate; APV, 2-amino-5-phosphopentanoate; PDF, probability density function; CNQX, 6-nitro-7-cyanoquinoxaline-2,3-dione.

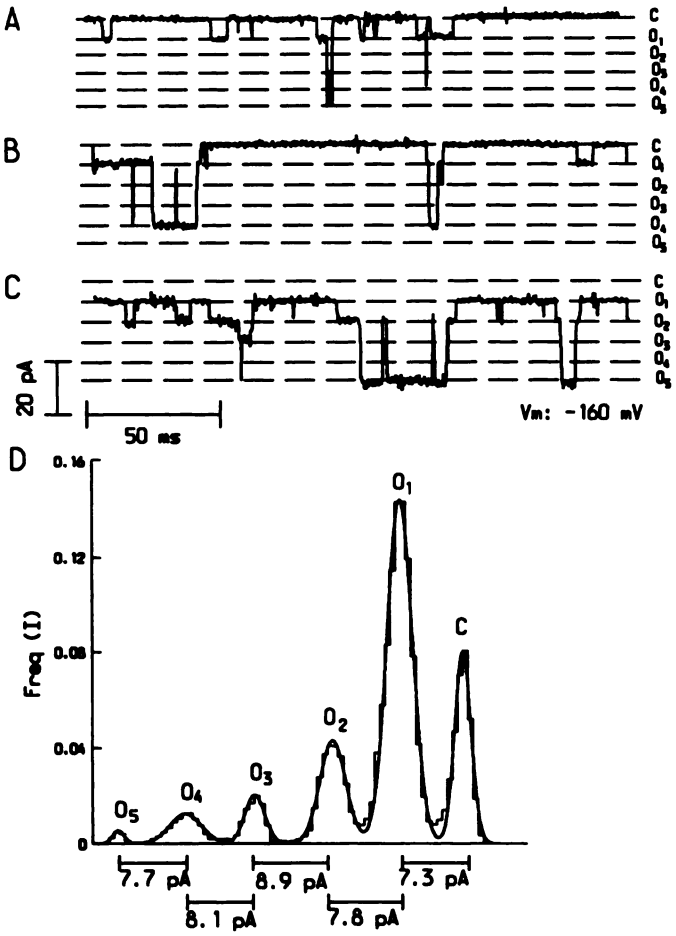

Fig. 1. A-C, Continuous recording of channel activity elicited from a bilayer containing total protein by 5×10^{-5} M NMDA (in the presence of 2×10^{-6} M glycine) at V_m of −150 mV, using the pipette-dipping technique. On playback, data were sampled at 10 kHz (100-μsec intervals) and low-pass filtered at 3 kHz. Openings are downwards. Various transitions between the closed state (*C*) and five open states (O_1-O_5) are apparent (A, C-O_1, O_1-O_4, O_1-O_5, O_3-O_5; B, C-O_1, C-O_2, O_1-O_4; C, O_1-O_2, O_2-O_3, O_2-O_4, O_2-O_5, O_3-O_5). D, Current amplitude ((I)) frequency histogram constructed from 120 sec of channel data exemplified in A-C. Channel data were low-pass filtered at 3 kHz and sampled at 50 kHz (20-μsec intervals) on playback. The five open channel conductance levels identified in the histogram give estimated conductance steps of 45.6 pS (probability $p = 0.52$) (O_1), 48.8 pS ($p = 0.16$) (O_2), 55.6 pS ($p = 0.06$) (O_3), 50.6 pS ($p = 0.06$) (O_4), and 47.9 pS ($p = 0.01$) (O_5).

showed high affinity binding of [^{3}H]kainate, [^{3}H]AMPA, and [^{3}H]glycine (strychnine insensitive). When the fractions were analyzed using sodium dodecyl sulfate-polyacrylamide gel electrophoresis, fraction I gave a double band at 42 kDa and fraction II an additional band at 100 kDa (19). The 42-kDa doublet and the 100-kDa band had a common immunoreactivity, which supports the contention that the former was present in both fractions. Additional details of the purification, separation, and identification procedures and results were described by Henley *et al.* (19).

The purified proteins (either total, fraction I, or fraction II) were incorporated into liposomes composed of 9 parts L-α-phosphatidylcholine (~17% L-α-asolectin, type IIS; Sigma) and 1 part cholesterol (grade 1; Sigma), as described elsewhere (20). They were then suspended in pipette saline, composed of 100 mM NaCl and 10 mM Tris citrate (pH 7.4), to give a final liposome concentration of 0.025% and a protein concentration of approximately 1.5 μg/ml. Electrophysiological studies were performed by introducing the receptor-containing liposomes into artificial bilayers of the same asolectin/cholesterol composition as that described above. Bilayers were formed by the apposition of two monolayers at the tip of patch pipettes, using the technique of pipette dipping (22). Patch pipettes were made from hard borosilicate glass capillaries (GC150-10; Clark Electromedical Instruments) using a three-pull technique (DMZ universal puller; Zeitz Instruments, Germany) and had tip resistances of 5–8 MΩ in saline. The seal resistance of a membrane bilayer formed by pipette dipping was typically 20 GΩ. Protein insertion into a bilayer was facilitated by using positive pipette potentials (V_m) of +180 mV for up to 60 min (in most cases channel activity was observed within a few minutes after membrane formation), after which time at least 50% of bilayers responded to one or more of AMPA, kainate, and NMDA. Bilayers were routinely transferred between different bath solutions using the sleeve technique of Quartararo and Barry (23). The bath solution contained 100 mM NaCl, 5 mM KCl, 2 mM $CaCl_2$, and 10 mM Tris-citrate (pH adjusted to 7.4 with HCl). Agonists [kainate, AMPA, NMDA (usually in the presence of glycine) and domoate], antagonists (CNQX, Mg^{2+}, Zn^{2+}, APV, and MK-801), and the plant lectin concanavalin A were dissolved in the bath saline.

Each bilayer was exposed to a single bath or a series of baths containing one of several different agonists at varying concentrations. Four kainate and AMPA concentrations within the range of 10^{-4} M to 10^{-7} M, four concentrations of domoate within the range of 10^{-5} M to 10^{-8} M, and 12 concentrations of NMDA within the range of 5×10^{-4} M to 5×10^{-7} M were used. NMDA was usually applied with glycine (either 10^{-6} M or 2×10^{-6} M). Those bilayers that failed to respond to the agonists were finally exposed to alamethicin (0.4–10 μg/ml). This peptide spontaneously inserts into lipid membranes to produce voltage-gated ion channels (24). The appearance of well defined alamethicin channels in a bilayer was taken as a good indicator of its structural integrity. In this manner, it was possible to assess reliably the success rate of the reconstitution experiments. Additional experiments were undertaken using the black lipid membrane technique (25). The results of these studies were qualitatively similar to those obtained with pipette dipping.

Single-channel data were recorded from the bilayers using a List EPC-7 patch-clamp amplifier connected to a Sony pulse code modulator PCM-701ES and standard video recorder. The polarity of all potentials (V_m) refers to that of the inside of the pipette in the case of pipette-dipping studies and the side connected to the headstage of the amplifier in the case of black lipid membrane studies. After analog to digital conversion, all data analyses were performed on a Masscomp MC5500 minicomputer. Current amplitude frequency histograms were constructed for a variety of membrane potentials by filtering the channel currents at 1–3 kHz and sampling at 50 kHz on playback. They were subsequently fitted by sums of Gaussian distributions using a nonlinear least-squares algorithm (Numerical Algorithm Group subroutine E04FDF). Where bilayers were studied over a range of potentials, peak amplitudes derived from the histograms were plotted against V_m; these plots were fitted by linear regression to give estimates of open channel conductances. Single-channel data were analyzed using the stringent criteria described in our previous publications (e.g., Ref. 26). Channel data were low-pass filtered at 3 kHz, with sampling at 10 kHz on playback, and a minimum dwell time of 0.1 msec was imposed. An automated procedure (27, 28) was used to measure single-channel open and closed times. Single-channel kinetics were characterized initially in terms of qualitative and quantitative changes in overall parameters [channel open probability (P_o), event frequency (f), mean open time (m_o), and mean closed time (m_c)] and then in terms of dwell-time (open and closed) PDFs.

Results

Membrane bilayers. Once formed, bilayers produced by the pipette-dipping technique were maintained for an average of 60 min, with some lasting up to 8 hr. The efficiency of the sleeve technique (23) as a method of transferring bilayers between different bath solutions was generally good, with >50% of patches surviving beyond one transfer. On average, each of these was taken through three or four transfers, with some bilayers surviving nine or 10 transfers.

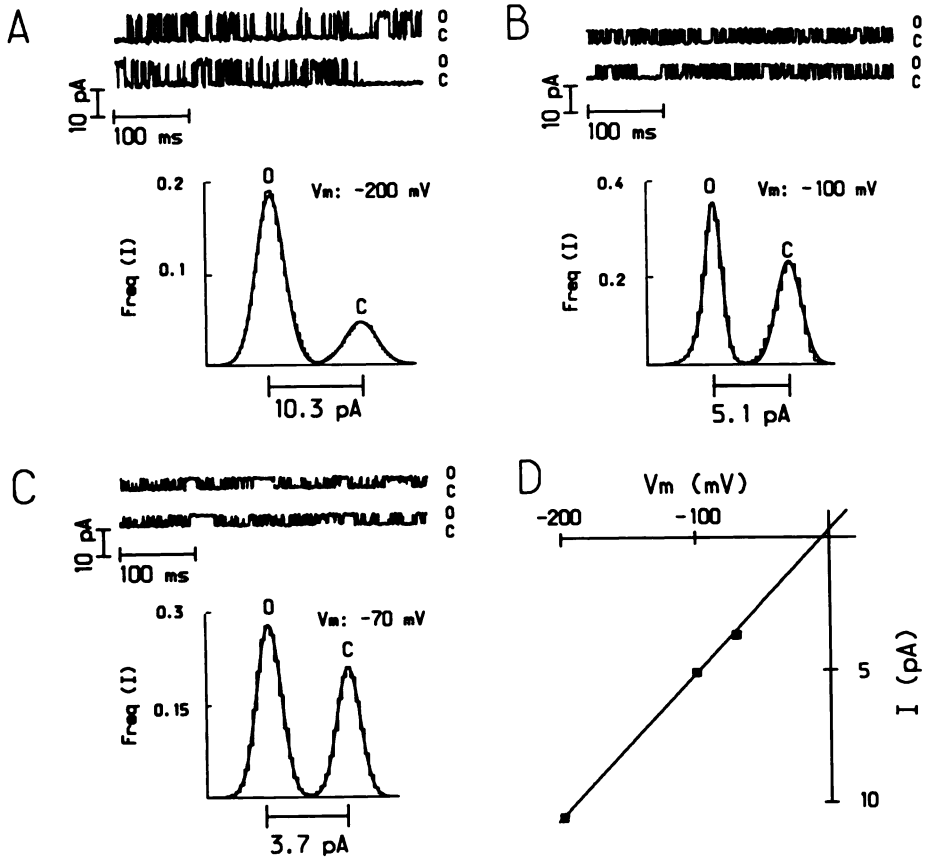

Fig. 2. Single-channel currents elicited by 10^{-5} M NMDA (in the presence of 2×10^{-6} M glycine) from a bilayer containing fraction II protein that gave a unitary conductance opening. A-C, Continuous recordings of channel activity at three different V_m values (A, −200 mV; B, −100 mV; C, −70 mV). Data were low-pass filtered at 3 kHz and sampled at 10 kHz (100-μsec intervals) on playback. Openings are upwards. The bilayers were formed using the pipette-dipping technique. Current amplitude ((I)) frequency histograms constructed from 60 sec of data in A-C are shown *below each set of recordings*. The data for the histograms were low-pass filtered at 3 kHz, with sampling at 50 kHz (20-μsec intervals). The histograms were fitted by sums of Gaussian distributions using a nonlinear least-squares algorithm. The peak amplitudes give estimated open channel conductance levels of 51.5 pS (A), 51 pS (B), and 53 pS (C). *O*, distribution of open channel currents: *C*, distribution of closed channel currents. D, The peak amplitudes (I) of the open channel current distibutions in A-C are plotted against V_m. The slope of the linear regression through the points on this plot is 52 pS.

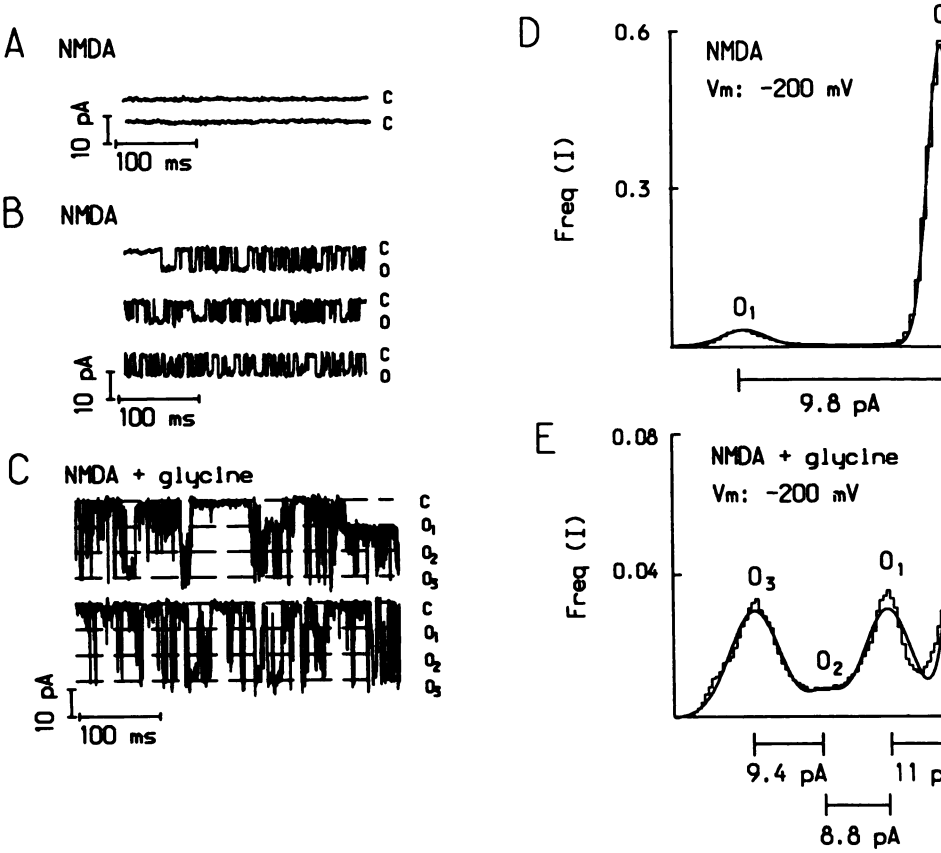

Fig. 3. A-C, Recordings from bilayers containing fraction II protein in response to 10^{-5} M NMDA in the absence (A and B) and presence (C) of 2×10^{-6} M glycine. The usual response to NMDA alone is shown in A; the response in B was seen on only five occasions in >500 tests. The recordings were made at V_m of −200 mV. Openings are downwards. Data were low-pass filtered at 3 kHz and sampled at 10 kHz (100-μsec intervals) on playback. The bilayer was formed using the pipette-dipping technique. O_1-O_3, open channel conductance levels; *C*, closed conductance level. D and E, Current amplitude ((I)) frequency histograms constructed from 50 sec of data exemplified in B and C, respectively. Data were low-pass filtered at 3 kHz, with sampling at 50 kHz (20-μsec intervals) on playback. The peak of the open channel current distribution in D gives a conductance of 49 pS. Three open channel conductance levels are present in E, i.e., 44 pS, 91 pS, and 146 pS.

TABLE 1

Channel openings gated by NMDA in three bilayers (A–C) containing total protein*

The data in A and B were obtained using the pipette-dipping technique; those in C were obtained using the black lipid membrane technique. V_m was −160 mV (A) or 100 mV (B and C).

	[NMDA]	N_e	m_o	m_c	P_o	f
	M		msec	msec		sec^{-1}
A.	5×10^{-6}	14,108	1.95	26.4	0.069	35.3
	5×10^{-5}	8,939	3.30	15.7	0.173	52.8
B.	10^{-6}	2,510	3.73	17.1	0.179	47.9
	10^{-5}	6,960	4.32	6.98	0.382	88.5
C.	10^{-4}	6,309	3.10	1.56	0.665	215

* N_e, number of events; m_o, mean channel open time; m_c, mean channel closed time; P_o, channel open probability; f, channel event frequency.

TABLE 2

Effect of Mg^{2+} concentration on channel openings gated by 10^{-5} M NMDA*

Data are from bilayers that contained total protein and were prepared using the pipette-dipping technique. V_m was −180 mV (zero Mg^{2+}) or −200 mV (10^{-3} M Mg^{2+}).

$[Mg^{2+}]$	N_e	m_o	m_c	P_o	f
M		msec	msec		sec^{-1}
0	5222	2.54	20.4	0.111	43.6
10^{-3}	125	0.96	2163	0.0005	0.46

* N_e, number of events; m_o, mean channel open time; m_c, mean channel closed time; P_o, channel open probability; f, channel event frequency.

Despite study of >1000 bilayers, channel openings were never seen when the bath contained saline alone, even when transmembrane potential differences of ±200 mV were imposed. With either kainate, AMPA, domoate, or NMDA, ~50% of bilayers containing total protein exhibited channel openings. When bilayers responsive to one or more of these agonists were transferred to a bath containing either γ-amino-*n*-butyric acid (n = 6 bilayers), acetylcholine (n = 6), or nicotine (n = 6) channel openings were not observed, even when the concentration of these ligands was as high as 10^{-4} M. Conversely, many bilayers that failed to respond to γ-aminobutyric acid, acetylcholine, or nicotine exhibited channel openings when they were transferred to a bath containing 10^{-5} M concentrations of either kainate, AMPA, domoate, or NMDA. In general, channel openings were continuously observed in the presence of the EAAs throughout the lifetime of a bilayer, although in some cases channel activity suddenly ceased and could not be reinitiated even when V_m was held at ±200 mV for periods of up to 1 hr. Bilayers that survived many transfers were usually exposed to one or more EAAs (kainate, AMPA, and NMDA) and antagonists (CNQX, Mg^{2+}, Zn^{2+}, APV, and MK-801). Some failed to respond to any of the EAAs, yet when they were exposed to alamethicin spontaneous channel openings appeared, i.e., in these cases the absence of EAAR channels was not due to the poor quality of the bilayers. The lectin concanavalin A (10^{-6} M) was applied to some bilayers that failed to respond to any of the EAAs, to test whether the absence of channel openings was due to EAAR desensitization. Concanavalin A is a selective inhibitor of desensitization of EAAR (29, 30). None of the bilayers treated with this lectin subsequently responded to EAAs.

Response of protein fractions. About 600 bilayers exposed to vesicles containing total protein were examined and 65% of these responded to one or more of either kainate, AMPA, or NMDA. The remaining 35% failed to respond to any of these agonists. Of ~200 membrane bilayers exposed to vesicles containing fraction I protein, 43% responded to AMPA and kainate and 57% failed to respond to any agonist; none of these bilayers responded to NMDA. Attempts made to elicit a response to NMDA from bilayers containing fraction I protein (the presence of this protein in the bilayers was known because they responded to applications of non-NMDA agonists), by raising either the NMDA concentration (to 10^{-4} M or 10^{-3} M) and/or the glycine concentration (to 10^{-4} M), were unsuccessful. Of ~200 membrane bilayers exposed to vesicles containing fraction II protein, about 85% responded to NMDA, kainate, and AMPA; the rest failed to respond to any of these agonists.

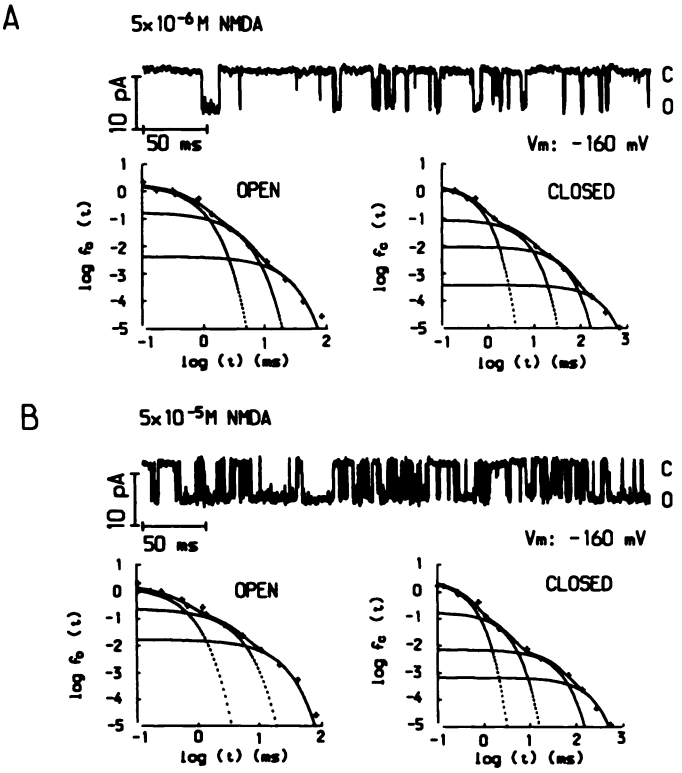

Fig. 4. Recordings of channel activity elicited from a bilayer containing total protein by 5×10^{-6} M NMDA (A) and 5×10^{-5} M NMDA (B), both plus 2×10^{-6} M glycine. Recordings were obtained at V_m of −160 mV using the pipette-dipping technique. Openings are downwards. On playback, data were sampled at 10 kHz (100-μsec intervals) and low-pass filtered at 3 kHz. PDFs for the data exemplified in A and B are shown *below the recordings* as log-log plots. +, Observed distributions; ——, fitted PDFs; – – –, individual exponential components of the fits. Histograms of openings were fitted by a three-exponential function. The time constants for the openings are 1.98 msec and 12.3 msec with 5×10^{-6} M NMDA (A) and 1.91 msec and 11.2 msec with 5×10^{-5} M NMDA (B). Histograms of closings were fitted by a four-exponential function. The time constants for the closings are 0.37 msec, 3.49 msec, 23.9 msec, and 173 msec for 5×10^{-6} M NMDA (A) and 0.25 msec, 1.62 msec, 22.6 msec, and 119 msec for 5×10^{-5} M NMDA (B).

NMDA-induced single-channel currents. The pharmacological responses of either reconstituted total protein or fraction II protein to NMDA and NMDAR antagonists were similar to those described in previous reports on NMDAR reconstituted into artificial lipid bilayers (31), NMDAR of cultured neurons (32), and NMDAR expressed in *Xenopus* oocytes injected with rat brain mRNA (4).

The majority (~80%) of recordings from these bilayers during NMDA application comprised multiple conductance levels, each ~50 pS (Fig. 1). In 10 bilayers only a single, ~50-pS, open channel conductance level was observed. Representative recordings from these bilayers are illustrated in Fig. 2, A-C, with

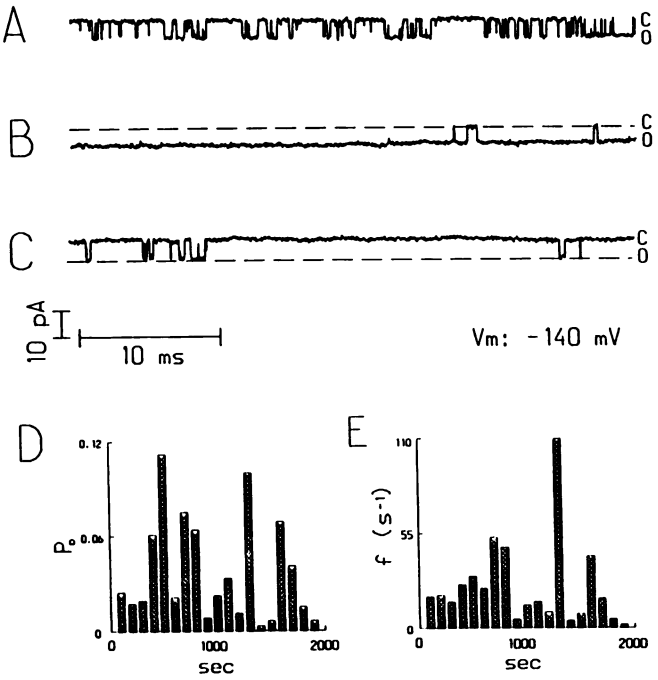

Fig. 5. A-C, Three sets of continuous traces of channel activity recorded from a bilayer containing total protein that was exposed to 10^{-6} M NMDA (in the presence of 2×10^{-6} M glycine) at −140 mV. Openings are downwards. In A the channel activity was characterized by rapid open-closed kinetics with brief openings (m_o = 1.32 msec) and brief closings (m_c = 3.40 msec). In B and C the open-closed kinetics were much slower, with long openings (B) (m_o = 19.8 msec) and long closings (C) (m_c = 11.2 msec). The bilayer was formed using the pipette-dipping technique. D and E, Bar plots showing variation in P_o (D) and f (E) as a function of time for a ~30-min recording of channel activity, in a bilayer containing total protein, elicited by 10^{-5} M NMDA (in the presence of 2×10^{-6} M glycine) at V_m of −100 mV. Each *bar* contains data for 100 sec of recording. Data in A-E were low-pass filtered at 3 kHz, with sampling at 10 kHz (100-μsec intervals) on playback.

their current amplitude frequency histograms. Here, channel activity was elicited by 10^{-5} M NMDA for three negative V_m values. When the peak open state current amplitudes of the histograms were plotted against V_m and the graph was fitted by linear regression, the slope of line gave an open channel conductance of 52 pS (Fig. 2D). Unfortunately, the data in Fig. 2 are rather limited and are restricted to the voltage range of −200 mV to −70 mV. Attempts to obtain equivalent data at more positive potentials were unsuccessful, so we do not know whether this channel rectifies. Howe *et al.* (33) reported that the I-V relationships for NMDAR channels of rat cerebellar granule cell neurons are nonlinear at holding potentials more negative than −100 mV. The NMDAR channel reconstituted from *Xenopus* CNS is seemingly different in this respect. The reason for this may become apparent when *in situ* studies of *Xenopus* NMDAR have been undertaken and when the structural properties of the subunits comprising these NMDAR are defined.

Channel openings were usually not elicited by NMDA in the absence of glycine (Fig. 3A). However, they were observed in a few bilayers (n = 5), but only with at least 10^{-6} M NMDA (Fig. 3B). The unitary single-channel openings present in the bilayer recording illustrated in Fig. 3B, which were observed in the absence of glycine, had a conductance of 49 pS (Fig. 3D). When this bilayer was exposed to 10^{-7} M NMDA and 2×10^{-6} M glycine, three open channel conductance levels were observed (Fig. 3, C and E). These were 44 pS, 47 pS, and 55 pS. We did not undertake a quantitative study of the effects of glycine concentration, but it seems that this cofactor increases f and P_o.

Bilayers varied considerably with respect to their responsiveness to NMDA (plus glycine) (Tables 1 and 2). In some (n = 5), typical NMDAR channel openings were elicited by 10^{-7} M NMDA (plus 2×10^{-6} M glycine), whereas in others (n = 6) 10^{-4} M NMDA (plus 2×10^{-6} M glycine) was required to elicit such activity. We have no explanation for this variability; it was not reduced when bilayers (n = 20) were pretreated with concanavalin A. The data contained in Fig. 4 and Table 1A were obtained from a single bilayer with two concentrations of NMDA (plus 2×10^{-6} M glycine), 5×10^{-6} M (Fig. 4A) and 5×10^{-5} M (Fig. 4B). P_o and f were increased by about 2.5-fold and 1.5-fold, respectively, and m_o was increased by about 1.7-fold when the concentration was raised 10-fold. Best fits to PDFs of channel open and closed times for these data required three- and four-exponential functions, respectively. Data from other bilayers (n = 6) gave similar results. It is of interest to note that Howe *et al.* (33, 34) reported similarly complex fits to PDFs for channels activated by NMDA in rat cultured neurons.

Some bilayers (n = 25) that responded to NMDA at positive V_m values failed to respond at negative V_m values. Also, in most recordings of activity elicited by NMDA the number of open channel conductance levels increased as V_m was made more positive. This may have been due to increases in f and m_o (35), although we do not have quantitative evidence to support this contention.

In all bilayers (n = 15) from which long term recordings were obtained, the activity elicited by NMDA was characterized by marked variations in P_o. This was due not only to variations of f but also to changes in m_o (see the legend to Fig. 5). The channel activity exemplified in Fig. 5 alternated between brief openings (m_o = 1.32 msec) and closings (m_c = 3.4 msec) on the one hand and long openings (m_o = 19.8 msec) and long closings (m_c = 11.2 msec) on the other hand. The marked changes in P_o and f that characterized this activity (Fig. 5, D and E) are strikingly reminiscent of those described for an invertebrate EAAR by Patlak *et al.* (36).

Low conductance openings gated by NMDA. Fig. 6 shows data obtained from a bilayer containing total protein that failed to respond to kainate but responded to NMDA. The response to NMDA comprised openings of ~9 pS in addition to characteristic openings of ~50 pS (Fig. 6A). Openings of ~9 pS were observed in response to NMDA in only two bilayers of a total of ~300 that responded to this ligand. The ~9-pS events were often seen superimposed upon ~50-pS openings, but recordings from both bilayers were too noisy to enable unequivocal identification of transitions between the closed state and a ~60-pS conductance level. The ~9-pS opening exhibited complex kinetics, i.e., similar to those of the ~50-pS opening described in Fig. 5. The addition of Mg^{2+} at 10^{-3} M eliminated the large conductance event at negative V_m values (not at positive V_m values) but did not affect the ~9-pS openings (Fig. 6B). Unfortunately, we were unable to test higher concentrations of Mg^{2+} because both bilayers were lost after the first test with this cation.

NMDAR antagonists. The effects of the classic NMDAR noncompetitive antagonists Mg^{2+} (as $MgCl_2$), Zn^{2+} (as $ZnSO_4$), and MK-801 (3, 6) and the competitive antagonist APV (37) on channels gated by NMDA were investigated. The three noncompetitive antagonists caused dose-dependent decreases

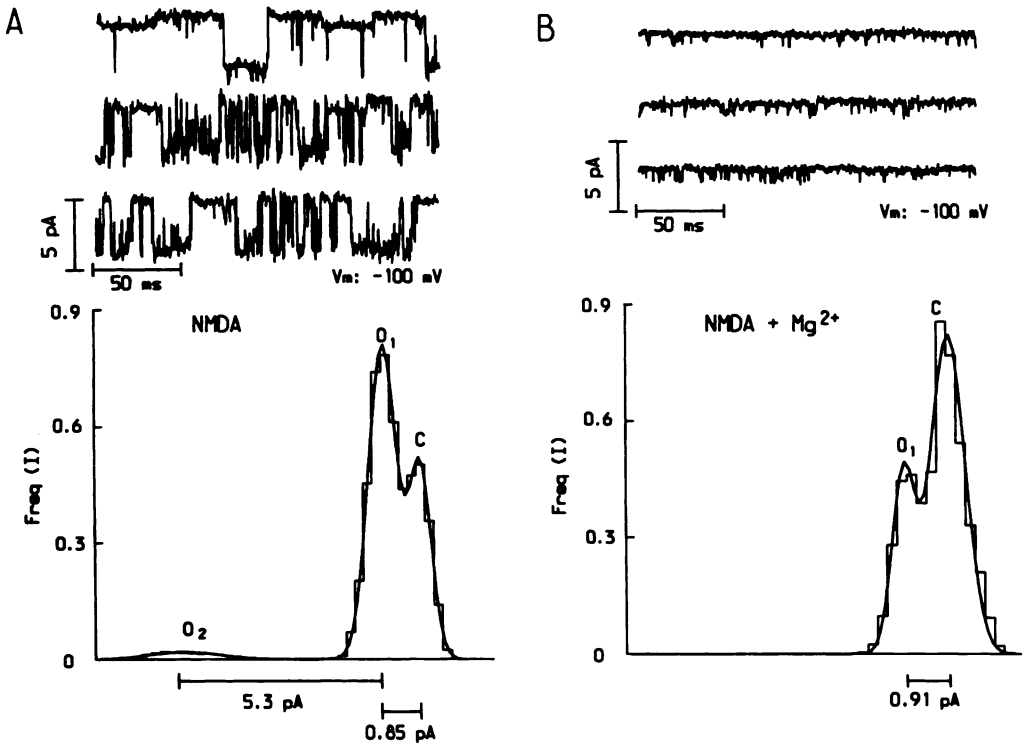

Fig. 6. Continuous recordings of channel activity elicited from a bilayer containing total protein by 10^{-5} M NMDA (in the presence of 2×10^{-6} M glycine) at V_m of −100 mV. The pipette-dipping technique was used. Channel openings are downwards. A, Mg^{2+} was absent; B, the bath saline contained 10^{-3} M Mg^{2+}. Data were low-pass filtered at 3 kHz, with sampling at 10 kHz (100-μsec intervals) on playback. Current amplitude ((I)) frequency histograms constructed from 60 sec of data are illustrated *below the recordings*. Data were low-pass filtered at 3 kHz, with sampling at 50 kHz (20-μsec intervals) on playback. The histogram in A identifies two open channel conductance levels, of 8.5 pS (O_1) and 53.5 pS (O_2). In B only a single open channel conductance level (O_1) is identified. *C*, distribution of closed channel currents in each case.

in P_o and m_o; in the case of Mg^{2+} and MK-801, antagonism was voltage dependent (3, 4, 38, 39). Zn^{2+} at 10^{-3} M and 5×10^{-6} M MK-801 (data not shown) reduced P_o to zero. The concentration of MK-801 that completely antagonizes NMDA responses at negative V_m values either *in situ* or in neuron cultures ranges from 7.5×10^{-8} M to 10^{-5} M, depending on the source (3, 40). The antagonism of NMDAR by 10^{-3} M Mg^{2+} was observed as characteristic brief interruptions (flickerings) of single-channel currents, which accounted for the decrease in m_o, in addition to reductions in P_o and f (Fig. 7A). Table 2 shows that not only were P_o and f greatly reduced (by about 250-fold and 100-fold, respectively) and m_c greatly increased (by about 100-fold) by 10^{-3} M Mg^{2+}, but m_o was also reduced (from 2.5 msec to 0.96 msec in the example illustrated in Fig. 7A). Flickerings were only observed at negative V_m values; at positive V_m values the activity was similar to that observed in the absence of the antagonist. A slightly higher concentration of Mg^{2+} completely antagonized NMDA-elicited channel activity at negative V_m values, but this antagonism could be relieved by making V_m positive (Fig. 7B). The Mg^{2+} concentrations used to achieve partial antagonism are similar to those reported for studies of Mg^{2+} antagonism of NMDAR of mouse neurons (38) and spinal neurons of rat (39). Notably, the addition of up to 10^{-2} M Mg^{2+} to bilayers responding to kainate and AMPA failed to block the channels gated by these EAAs at either negative or positive V_m values.

APV at 10^{-6} M to 5×10^{-6} *m.* reduced P_o, f, and m_o for channels gated by 10^{-5} M NMDA (Table 3); channel openings were completely antagonized by 10^{-5} M APV (Fig. 7C, compare *upper* and *middle traces*). However, if the concentration of NMDA was then increased to 10^{-4} M in the presence of 10^{-5} M APV, the antagonism elicited by APV was relieved (Fig. 7C, *lower trace*). The competitive and voltage-independent interaction between NMDA and APV distinguishes antagonism of NMDAR by the latter from that by either Mg^{2+} or MK-801. CNQX (10^{-5} M) had no effect on NMDA-induced channel activity.

Channels induced by kainate. With most bilayers that responded to kainate, at 10^{-7} to 10^{-4} M this amino acid usually elicited a number of open conductance levels, with the smallest being about ~9 pS (Fig. 8A; see also Fig. 11A). Transitions between all levels seemed to be present in recordings from these bilayers, but it was not possible, because of noise, to determine unequivocally whether the higher conductances result from simultaneous openings of more than one ~9-pS channel or whether kainate gates channels of different conductances. In two bilayers (of a total of ~500 that responded to kainate) a single open channel conductance level was observed, suggesting possibly the presence of a single active channel in the bilayer. The data obtained from these two bilayers were similar qualitatively and quantitatively. Fig. 9A shows a current amplitude histogram for one such bilayer, in which the channels had a conductance of 9.4 pS; this is comparable to the primary channel conductance activated by kainate in cerebellar granule cells (41). Further quantitative kinetic analysis of the data exemplified in Fig. 9A, which were obtained in the presence of 5×10^{-5} M kainate at V_m of −130 mV, gave a m_o of 1.07 msec and a m_c of 3.15 msec. Best fits to PDFs of channel open and closed times for these data required three- and four-exponential functions, respectively (Fig. 10A and B). The time constants for the openings were 0.21 msec, 0.81 msec, and 3.6 msec; those for closings were 0.22 msec, 1.4 msec, 5.1 msec, and 64.3 msec. Similarly complex fits have been reported for channels activated by glutamate, quisqualate, and kainate in cultured rat cerebellar granule cells (41).

KAINR antagonists. CNQX is a potent competitive antagonist of KAINR (42). The response to kainate of dorsal horn neurons in rat spinal cord (42) is reduced by about 50% by 10^{-3} M CNQX. However, Sucher *et al.* (43) found that 10^{-5} M CNQX reduced the kainate response of rat retinal ganglion cells by

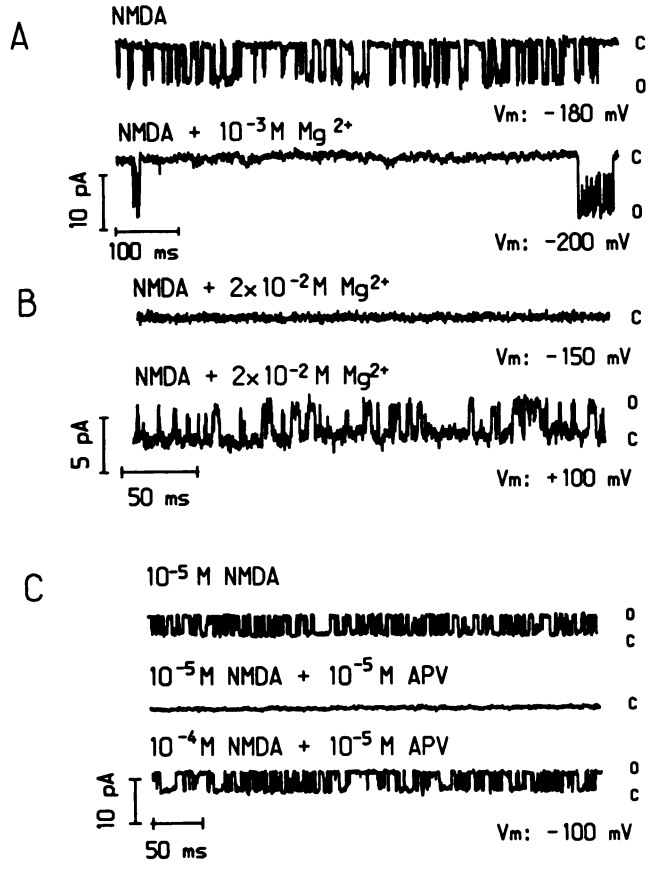

Fig. 7. A and B, Recordings of channel activity elicited from a bilayer containing total protein by 5×10^{-6} M NMDA (A) and by 10^{-5} M NMDA (B) in the presence of 2×10^{-6} M glycine. Openings are downwards in A and upwards in B and C. A, Recordings made using the pipette-dipping technique at V_m of −180 mV (*upper trace*) and V_m of −200 mV (*lower trace*). In the absence of Mg^{2+}, m_o = 2.5 msec (*upper trace*); in the presence of 10^{-3} M Mg^{2+}, flickering block is seen (*lower trace*); m_o (0.96 msec) and P_o were reduced, compared with control. Total block of the NMDA-induced channel activity in this bilayer was achieved with 5×10^{-3} M Mg^{2+}. The recordings in B were made using the black lipid membrane technique. NMDA-induced channel openings were completely abolished by 2×10^{-2} M Mg^{2+} at V_m of −150 mV (B, *upper trace*), but antagonism was relieved when the membrane potential was changed to V_m of +100 mV. C, Recordings of channel activity elicited from a bilayer containing total protein by 10^{-5} M NMDA (in the presence of 2×10^{-6} M glycine). The bilayer was formed using the pipette-dipping technique. Channel currents are downwards. Data were recorded at V_m of −100 mV. *Upper trace*, recording obtained in the absence of APV. Total block of channel openings was obtained with 10^{-5} M APV (*middle trace*). This antagonism was relieved by increasing the concentration of NMDA to 10^{-4} M (*lower trace*). On playback, data were sampled at 10 kHz (100-μsec intervals) and low-pass filtered at either 3 kHz (A and C) or 1 kHz (B).

TABLE 3

Effect of APV concentration on channel openings gated by 10^{-5} M NMDA in bilayers containing total protein*

The bilayers were formed using the pipette-dipping technique. V_m was −100 mV.

[APV]*	N_e	m_o	m_c	P_o	f
M		msec	msec		sec^{-1}
0	3280	1.98	2.14	0.482	243
10^{-6}	8180	1.08	3.80	0.221	205
5×10^{-6}	593	0.95	15.9	0.057	57.0

* N_e, number of events; m_o, mean channel open time; m_c, mean channel closed time; P_o, channel open probability; f, channel event frequency.

90%. The potency of this antagonist is clearly quite variable. The concentrations of CNQX used in our studies to produce partial antagonism of a response to kainate are similar to those used by Honoré and colleagues (42, 44) in their studies of cultured mouse cortical neurons, by Randle *et al.* (45) in *Xenopus* oocytes injected with rat cortex mRNA, and by Collingridge and colleagues (46, 47) in their studies of KAINR in rat hippocampus. The channel activity illustrated in Fig. 11A was elicited by 10^{-5} to 10^{-4} M kainate and comprised multiple conductance levels. It was reduced to a single open channel conductance level of ~9 pS by 10^{-5} M CNQX (Fig. 11B) and was abolished by 5×10^{-5} M CNQX (Fig. 11C). If the concentration of kainate was increased 5-fold after channel activity had been abolished with CNQX, the antagonism elicited by CNQX was relieved (Fig. 11D). Concentrations of Mg^{2+} and Zn^{2+} as high as 10^{-2} M did not antagonize activity elicited by kainate.

Channels induced by AMPA. Channel activity induced by 10^{-7} M to 10^{-4} M AMPA usually (n = 21) comprised multiple conductance levels, in which ~6-pS events were clearly present (Fig. 8B). As with kainate, transitions between all conductance levels may have occurred, but the recordings were too noisy to enable unequivocal identification of such transitions. In other words, it is possible that the higher conductance levels resulted from simultaneous openings of two or more channels of ~6 pS, although unitary openings of conductances higher than 6 pS may also have been present. Fig. 9B shows an example of a single channel with a conductance of ~6 pS that was activated by AMPA. Quantitative kinetic analysis of this channel at −160 mV gave a m_o of 0.54 msec and a m_c of 1.47 msec. Best fits to PDFs of channel open times required only two-exponential functions, with time constants of 0.34 msec and 1.4 msec (Fig. 10C) and with the faster component contributing the greater proportion of events (p = 0.93), i.e., more than that contributed by the fastest component of the unitary conductance channel evoked by kainate (p = 0.49) (48). Best fits to PDFs for channel closed times required three-exponential functions, with time constants of 0.77 msec, 1.6 msec, and 9.3 msec (Fig. 10D). Concentrations of Mg^{2+} or Zn^{2+} as high as 10^{-2} M had no effect on AMPA-induced channel openings, but AMPA-induced activity was antagonized by CNQX.

Channels induced by domoate. Channel openings of 9–10 pS were induced with domoate at concentrations as low as 10^{-8} M. Neither 10^{-2} M Mg^{2+} nor 3×10^{-5} M MK-801 affected channel activity elicited by domoate. However, it was antagonized by 10^{-6} M 2,3-dihydroxy-6,7-dinitroquinoxaline, an analogue of CNQX.

Cross-reactions. Channel openings elicited by NMDA in bilayers containing fraction II protein were antagonized by 1 mM Mg^{2+}, whereas those elicited by kainate (in the absence of NMDA) were not antagonized even by 10 mM Mg^{2+}. However, when kainate (or AMPA) and NMDA were applied together to two bilayers containing fraction II protein, 10^{-3} M Mg^{2+} blocked all channel activity at negative V_m, despite the fact that it had no effect in these bilayers on the activity evoked by kainate application alone. In other bilayers containing fraction II protein a proportion of the channel openings gated by joint application of kainate and NMDA were not antagonized by Mg^{2+}. Mg^{2+} at 10^{-2} M had no effect on the response to joint application of kainate and NMDA in bilayers containing fraction I protein, i.e., the protein fraction that was not responsive to NMDA.

High conductance channels. Some batches (two of 25) of

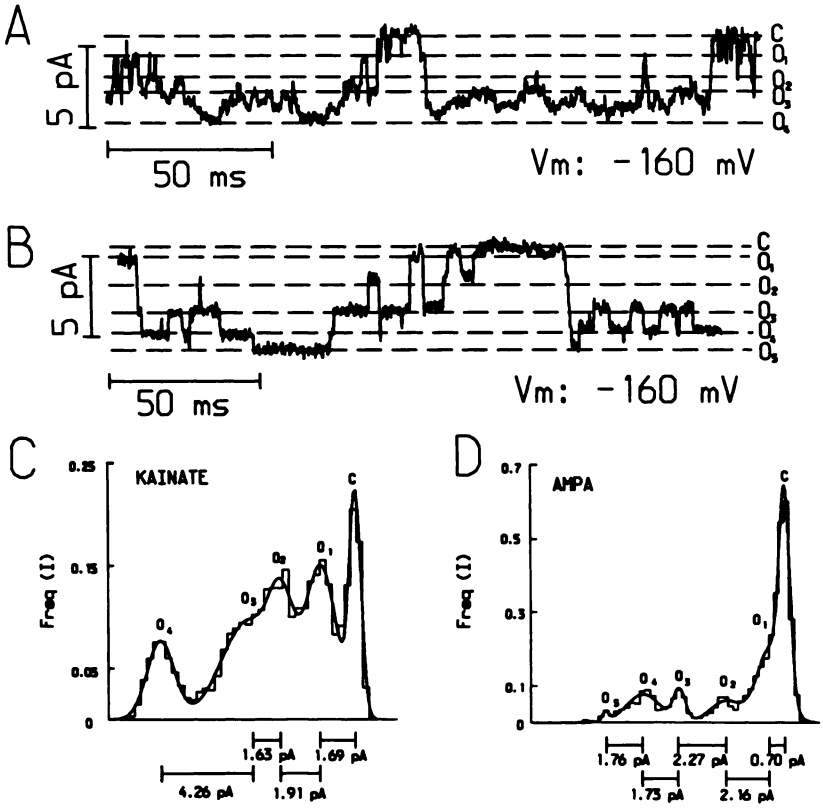

Fig. 8. A and B, Recordings of channel activity elicited from bilayers containing fraction II protein by 10^{-5} M kainate at −160 mV (A) and from bilayers containing fraction I protein by 10^{-5} M AMPA at −160 mV (B). Openings are downwards in both records. The bilayers were formed using the pipette-dipping technique. *C*, zero current, i.e., the closed channel conductance level. Channel data were low-pass filtered at 3 kHz and sampled at 10 kHz (100-μsec intervals) on playback in both A and B. C and D, Current amplitude ((I)) frequency histograms constructed from 90 sec (C) and 60 sec (D) of data exemplified in A and B, respectively. Data for histograms were low-pass filtered at 1 kHz, with sampling at 50 kHz (20-μsec intervals) on playback. Open channel conductance levels estimated from the peaks of the histogram in C are 10.6 pS (p = 0.33) (O_1), 22.5 pS (p = 0.15) (O_2), 32.7 pS (p = 0.37) (O_3), and 59.3 pS (p = 0.15) (O_4). Open channel conductance levels estimated from the histogram in D are 4.4 pS (p = 0.5) (O_1), 17.9 pS (p = 0.16) (O_2), 32.1 pS (p = 0.09) (O_3), 42.9 pS (p = 0.23) (O_4), and 53.9 pS (p = 0.02) (O_5).

protein behaved atypically when reconstituted and exposed to NMDA and non-NMDA agonists. For example, ~400-pS unitary channel openings were observed with NMDA (Fig. 12A), whereas with AMPA open channel conductance levels of ~24 pS or higher were seen (Fig. 12B). Sometimes these high conductance openings occurred in addition to the typical conductance events expected for these amino acids, but in other cases only atypical openings were present. Although the conductances of the NMDA-elicited channel openings were much higher than expected, they still exhibited the pharmacological properties associated with NMDAR, whereas the high conductance channels gated by kainate (and AMPA and domoate) had agonist/antagonist properties typical of those associated with non-NMDAR. For example, in one bilayer, where a unitary ~150-pS channel conductance level was observed with 10^{-5} M NMDA, 10^{-3} M Mg^{2+} induced partial, voltage-dependent antagonism, seen as brief interruptions (flickerings) of the ~150-pS single-channel current, in addition to reductions in P_o and f; 5×10^{-3} M Mg^{2+} completely antagonized the NMDA-induced activity, but only at negative V_m values. In another bilayer, where multiple channel conductance levels, each of ~28 pS, were observed with 10^{-5} M kainate, 10^{-5} M CNQX partially antagonized the kainate-induced activity, i.e., the number of ~28-pS conductance levels was reduced from three to one. Antagonism was complete with 5×10^{-5} M CNQX. In neither case was partial antagonism associated with a decrease in the unitary conductance of the open channel such that ~9-pS (with kainate) or ~50-pS (with NMDA) step reductions were observed.

Discussion

Using domoate affinity chromatography we have demonstrated that in membrane bilayers incorporating *Xenopus* brain proteins, either total protein or fraction II protein, channel activity could be induced by NMDA, kainate, and AMPA. Henley *et al.* (19) have shown that the total protein and fraction II contain a ~42-kDa polypeptide and a 100-kDa polypeptide. In contrast, only kainate and AMPA gated channels in membranes containing fraction I protein; this fraction was shown to contain only polypeptides of 42-kDa apparent molecular mass (19).

The retention on the domoate (or AMPA or kainate) column of *Xenopus* EAAR that exhibit characteristic NMDAR pharmacology and physiology is surprising, because domoate binds extremely weakly at NMDAR agonist binding sites in amphibian brain (19). An explanation for this finding is that some EAAR of *Xenopus* CNS may be chimeras of NMDAR and non-NMDAR. The effect of Mg^{2+} on fraction II protein suggests that such chimeras may gate a common ion channel. This idea receives additional credibility from the recent work by Brackley and Usherwood (49) on *Xenopus* oocytes injected with *Xenopus* CNS mRNA. However, *in situ* studies of glutamate receptors of *Xenopus* CNS will be required to test the chimera hypothesis.

The finding that single-channel recordings from glutamate receptors of mammalian central neurons, using pipettes containing L-glutamate, sometimes contain small (5–15-pS), intermediate (20–35-pS), and large (40–50-pS) open channel conductances has been commonly reported, but the intermediate (20–35-pS) conductances are usually rare (50, 51). NMDA elicits primarily large conductance openings, although small and intermediate conductance openings have been observed with this agonist. NMDA-induced openings other that those of ~50 pS were seen only rarely in our studies. However, in two bilayers NMDA gated a ~9-pS conductance opening in addition to a characteristic ~50-pS opening. We have been unable either to confirm or to deny unequivocally the presence of unitary

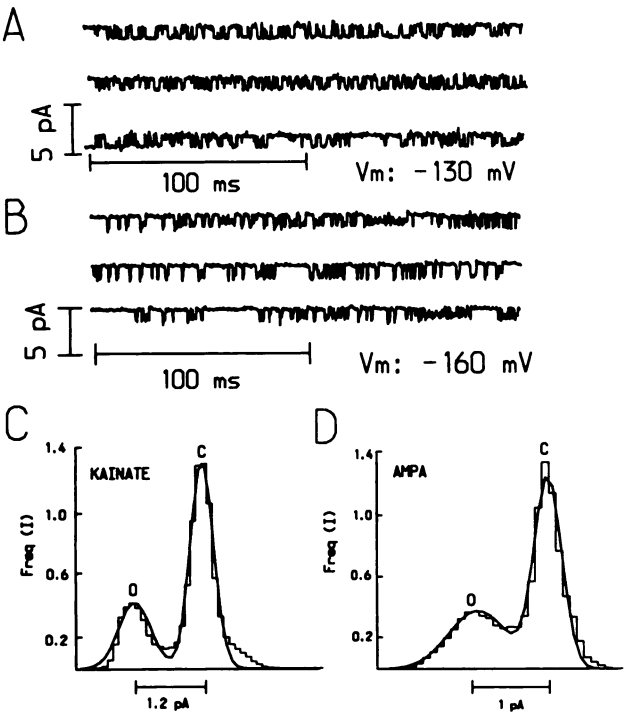

Fig. 9. A and B, Recordings of single-channel activity from bilayers containing fraction II protein (A) and fraction I protein (B). The activity was elicited by 5×10^{-5} M kainate at V_m of −130 mV (A) and 10^{-5} M AMPA at V_m of −160 mV (B). Channel openings are downwards. The bilayers were made using the pipette-dipping technique. The channel data were low-pass filtered at 3 kHz and sampled at 10 kHz (100-μsec intervals) on playback. C and D, Current amplitude ((I)) frequency histograms constructed from 60 sec of the channel data exemplified in A and B, respectively. The data for the histograms were low-pass filtered at 1 kHz and sampled at 50 kHz (20-μsec intervals) on playback. The histograms give estimated single-channel conductances of 9.4 pS ($p = 0.3$) for kainate and 6.3 pS ($p = 0.4$) for AMPA.

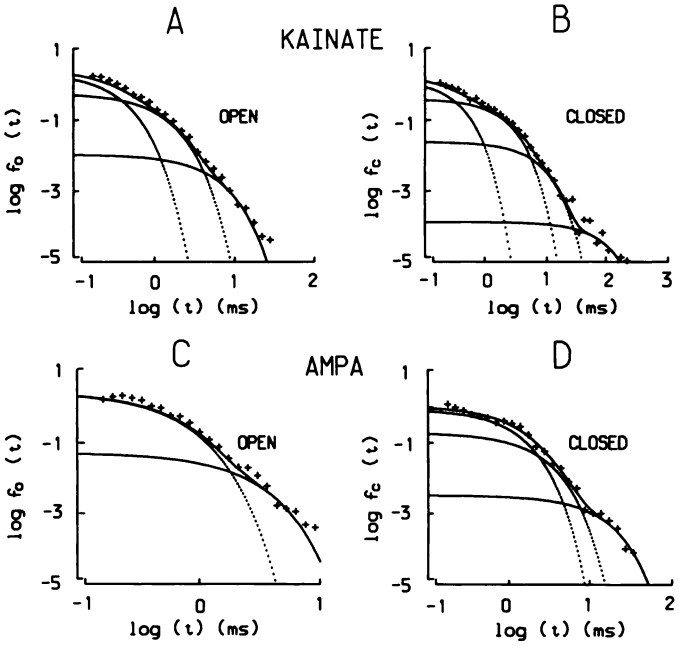

Fig. 10. Log-log PDFs for channel data exemplified in Fig. 9, C and D. +, Observed distributions; ——, fitted PDFs; – – –, individual exponential components of the fits. PDFs of channel openings were fitted by either three-exponential (for kainate (A)) or two-exponential (for AMPA (C)) functions, whereas PDFs for channel closings were fitted by four-exponential (for kainate (B)) and three-exponential (for AMPA (D)) functions. The time constants of the open PDF fits are 0.21 msec ($p = 0.49$), 0.81 msec ($p = 0.47$), and 3.6 msec ($p = 0.04$) for 10^{-5} M kainate (A) and 0.34 msec ($p = 0.93$) and 1.4 msec ($p = 0.07$) for 10^{-5} M AMPA (B). The time constants of the closed PDF fits are 0.22 msec ($p = 0.30$), 1.4 msec ($p = 0.57$), 5.1 msec ($p = 0.12$), and 64.3 msec ($p = 0.01$) for kainate (A) and 0.77 msec ($p = 0.67$), 1.6 msec ($p = 0.30$), and 9.3 msec ($p = 0.03$) for AMPA.

openings of ~60 pS in these recordings, so we have not eliminated the possibility that the ~9-pS event is a unitary opening, even perhaps of a non-NMDAR channel. The failure to block the ~9-pS event with 5 mM Mg^{2+} provides some support for this latter possibility, although a subconductance state of a NMDA channel might be less sensitive to Mg^{2+} block than a ~50-pS opening of this channel. The multiple conductance activity elicited by kainate and AMPA may have contained some intermediate and large conductance unitary channels of the type recorded from vertebrate neurons, but such openings were not observed in the few recordings obtained with non-NMDA agonists in which only a single channel appeared to be active. It seems likely that the multiple conductance levels observed in most recordings with kainate and AMPA resulted from openings of a number of ~9-pS or ~6-pS channels, respectively.

The strategy that we have used for the incorporation of purified EAAR proteins into artificial membranes has proved to be reasonably successful, and the single-channel data that have been obtained from the reconstituted proteins are similar in many respects to those obtained from vertebrate EAAR *in situ*. However, bilayers containing receptors reconstituted from some batches of *Xenopus* protein were consistently characterized by agonist-induced channel openings of abnormally high conductances. A likely explanation for this is that these batches of protein reconstituted into the bilayers as functional aggregates. This predisposition for aggregation was clearly due to

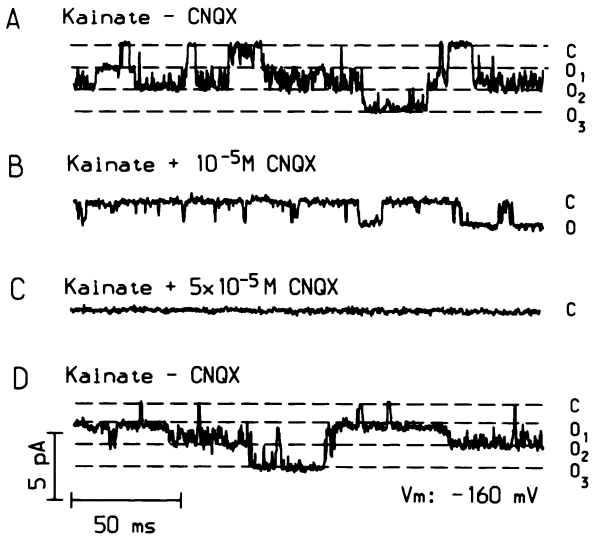

Fig. 11. Recordings of channel activity elicited from a bilayer containing fraction II protein by 10^{-5} M kainate. Openings are downwards. The bilayer was formed using the pipette-dipping technique. A, Multiple open channel conductance levels characterized the recording obtained in the absence of CNQX. B-D, Antagonism of channel openings by CNQX. The antagonism was incomplete with 10^{-5} M CNQX (B). CNQX at 5×10^{-5} M completely antagonized the kainate-induced channel activity (C). After removal of CNQX, the activity induced by kainate reappeared (D). Data were recorded at −160 mV and low-pass filtered at 2 kHz, with sampling at 10 kHz (100-μsec intervals) on playback. The response of this bilayer to AMPA was similarly antagonized by CNQX (data not shown).

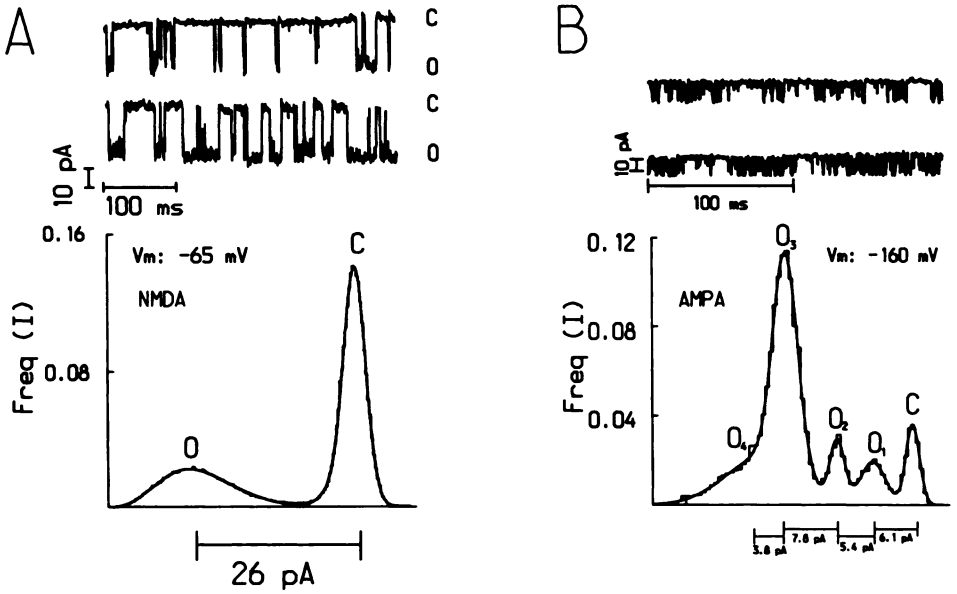

Fig. 12. Recordings of apparently unitary, high conductance, channel openings elicited by 10^{-5} M NMDA (plus 2×10^{-6} M glycine) (A) and by 10^{-5} M AMPA (B), obtained from a bilayer containing total protein. The current amplitude ((I)) frequency histograms illustrated *below these recordings* were constructed from 30 sec of data exemplified in the *traces*. Estimated open channel conductance levels are 400 pS for NMDA and 24 pS ($p = 0.28$), 34 pS ($p = 0.07$), 38 pS ($p = 0.09$), and 49 pS ($p = 0.46$) for AMPA. Data for histograms were filtered at 1 kHz and sampled at 50 kHz (20-μsec intervals).

some property of the protein rather than of the bilayer. Receptor aggregation might occur during detergent removal from the purified protein before it is reconstituted into lipid (52). It has been previously proposed by Schurholz *et al.* (53) and Schindler *et al.* (54) that aggregated receptor proteins cooperatively open and close their constituent channels. Although there is also some evidence for this phenomenon in native membranes (55, 56), it does not relate to EAAR in vertebrate CNS.

Recent studies using *in vitro* preparations indicate that NMDAR undergo a use-dependent decline in responsiveness during prolonged exposure to agonist, i.e., desensitization (30). In our studies we did not undertake a systematic search for desensitization. However, in bilayers with a single active NMDAR, multiple-exponential fits were required for the closed time PDFs, and one (or more) of these components may have been associated with a desensitized state of NMDAR. The majority of bilayers that responded to NMDA exhibited multiple conductance levels, which would have made desensitization difficult to identify.

This detailed account of single-channel data recorded from EAAR reconstituted into artificial bilayers raises interesting questions, the answers to some of which may lie in the procedures used to isolate and purify the receptor proteins. The next step will be to investigate EAAR of *Xenopus* CNS *in situ*, using whole-cell and single-channel recording techniques, in an attempt to determine whether the postulated chimeric NMDAR/non-NMDAR also exist *in vivo*.

References

1. Monaghan, P. T., R. J. Bridges, and C. W. Cotman. The excitatory amino acid receptors: their classes, pharmacology, and distinct properties in the function of the central nervous system. *Annu. Rev. Pharmacol. Toxicol.* **29**:365–402 (1989).
2. Watkins, J. C., P. Krogsgaard-Larsen, and T. Honoré. Structure-activity relationships in the development of excitatory amino acid receptor agonists and competitive antagonists. *Trends Pharmacol. Sci.* **11**:25–33 (1990).
3. Wong, E. H. F., J. A. Kemp, T. Priestley, A. R. Knight, G. N. Woodruff, and L. L. Iversen. The anticonvulsant MK-801 is a potent *N*-methyl-D-aspartate antagonist. *Proc. Natl. Acad. Sci. USA* **83**:7104–7108 (1986).
4. Verdoorn, T. A., N. W. Kleckner, and R. Dingledine. Rat brain *N*-methyl-D-aspartate receptors expressed in *Xenopus* oocytes. *Science* **238**:1114–1116 (1987).
5. Ascher, P. Magnesium block of the NMDA receptor channel, in *Neurology and Neurobiology. Frontiers in Excitatory Amino Acid Research* (E. A. Cavalheiro, J. Lehman, and L. Turshi, eds.). Alan R. Liss Inc., New York, 151–157 (1988).
6. Westbrook, G. L., and M. L. Mayer. Micromolar concentrations of Zn^{2+} antagonize NMDA and GABA responses of hippocampal neurons. *Nature (Lond.)* **328**:640–643 (1987).
7. Barnard, E. A., and J. Henley. The non-NMDA receptors: types, protein structure and molecular biology. *Trends Pharmacol. Sci.* **11**:500–508 (1990).
8. Hollmann, M., A. O'Shea-Greenfield, S. W. Rogers, and S. Heinemann. Cloning by functional expression of a member of the glutamate receptor family. *Nature (Lond.)* **342**:643–648 (1989).
9. Moriyoshi, K., M. Masu, T. Ishii, R. Shigemoto, N. Mizuno, and S. Nakanishi. Molecular cloning and characterisation of the rat NMDA receptor. *Nature (Lond.)* **354**:31–37 (1991).
10. Boulter, J., M. Hollman, A. O'Shea-Greenfield, M. Hartley, E. Deneris, C. Maron, and S. Heinemann. Molecular cloning and functional expression of glutamate receptor subunit genes. *Science* **249**:1033–1037 (1990).
11. Keinanen, K., W. Wisden, B. Sommer, P. Werner, A. Herb, T. A. Verdoorn, B. Sakmann, and P. H. Seeburg. A family of AMPA-selective glutamate receptors. *Science* **249**:556–560 (1990).
12. Nakanishi, N., N. A. Shneider, and R. Axel. A family of glutamate receptor genes: evidence for the formation of heteromultimeric receptors with distinct channel properties. *Neuron* **5**:569–581 (1990).
13. Sakimura, K., H. Bujo, E. Kushiya, K. Araki, M. Yamazaki, M. Yamazaki, H. Meguro, A. Verashina, S. Numa, and M. C. Mishina. Functional expression from cloned cDNA's of glutamate receptor species responsive to kainate and quisqualate. *FEBS Lett.* **272**:73–80 (1990).
14. Werner, P., M. Voigt, K. Keinanen, W. Wisden, and P. H. Seeberg. Cloning of a putative high-affinity kainate receptor expressed predominantly in hippocampal CA3 cells. *Nature (Lond.)* **351**:742–744 (1991).
15. Egebjerg, J., B. Bettler, I. Hermans-Borgmeyer, and S. Heinemann. Cloning of a cDNA for a glutamate receptor subunit activated by kainate but not AMPA. *Nature (Lond.)* **351**:745–748 (1991).
16. Hume, R. I., R. Dingledine, and S. F. Heinemann. Identification of a site in glutamate receptor subunits that controls calcium permeability. *Science* **253**:1028–1031 (1991).
17. London, E. D., N. Klemm, and J. T. Coyle. Phylogenetic distribution of [^{3}H] kainic acid receptor binding sites in neuronal tissue. *Brain Res.* **192**:463–476 (1980).
18. Hampson, D. R., D. Huie, and R. J. Wenthold. Properties of stabilized kainic acid binding sites for rat and frog brain. *J. Neurochem.* **48**(suppl.):537D (1987).
19. Henley, J. M., A. Ambrosini, D. Rodriguez-Ithurralde, H. Sudan, P. Brackley, C. Kerry, I. Mellor, K. Abutidze, P. N. R. Usherwood, and E. A. Barnard. Purified unitary kainate/α-amino-3-hydroxy-5-methylisooxazole-propionate (AMPA) and kainate/AMPA/*N*-methyl-D-aspartate receptors with interchangeable subunits. *Proc. Natl. Acad. Sci. USA* **89**:4806–4810 (1992).
20. Henley, J. M., and E. A. Barnard. Kainate receptors in *Xenopus* central nervous system: solubilisation with *N*-octyl-β-D-glucopyranoside. *J. Neurochem.* **52**:31–37 (1989).
21. Slevin, J. T., J. F. Collins, K. Lindsley, and J. T. Coyle. Analogue interactions with brain receptor labelled by [^{3}H]kainic acid. *Brain Res.* **265**:169–172 (1983).
22. Coronado, R., and R. Latorre. Phospholipid bilayers made from monolayers on patch-clamp pipettes. *Biophys. J.* **43**:231–236 (1983).
23. Quartararo, N., and P. H. Barry. A simple technique for transferring excised patches of membrane to different solutions for single channel measurements. *Pflügers Arch.* **410**:677–678 (1987).
24. Fox, R. O., Jr., and F. M. Richards. A voltage-gated ion channel model inferred from the crystal structure of alamethicin at 1.5-Å resolution. *Nature (Lond.)* **300**:325–330 (1982).

25. Montal, M., and P. Mueller. Formation of bimolecular membranes from lipid monolayers and a study of their electrical properties. *Proc. Natl. Acad. Sci. USA* **69**:3561–3566 (1972).
26. Kerry, C. J., R. L. Ramsey, M. S. P. Sansom, and P. N. R. Usherwood. Glutamate receptor-channel kinetics: the effect of glutamate concentration. *Biophys. J.* **53**:39–52 (1988).
27. Gration, K. A. F., J. J. Lambert, R. L. Ramsey, R. P. Rand, and P. N. R. Usherwood. Closure of membrane channels by glutamate receptors may be a two-step process. *Nature (Lond.)* **295**:599–601 (1982).
28. Kerry, C. J., K. S. Kits, R. L. Ramsey, M. S. P. Sansom, and P. N. R. Usherwood. Single channel kinetics of a glutamate receptor. *Biophys. J.* **51**:137–144 (1987).
29. Mathers, D. A., and P. N. R. Usherwood. Effects of concanavalin A on junctional and extrajunctional L-glutamate receptors on locust skeletal muscle fibres. *Comp. Biochem. Physiol. C Comp. Pharmacol.* **59**:151–155 (1978).
30. Mayer, M. L., and L. Vyklicky, Jr. Concanavalin A selectively reduces desensitization of mammalian neuronal quisqualate receptors. *Proc. Natl. Acad. Sci. USA* **86**:1411–1415 (1989).
31. Vodyanoy, V., D. Muller, K. Kramer, G. Lynch, and M. Baudry. Functional reconstitution of *N*-methyl-D-aspartate receptors in artificial lipid bilayers. *Neurosci. Lett.* **81**:133–138 (1987).
32. Cull-Candy, S. G., and M. M. Usowicz. Multiple conductance single channels activated by excitatory amino acids in cerebellar neurons. *Nature (Lond.)* **325**:525–528 (1987).
33. Howe, J. R., S. G. Cull-Candy, and D. Colquhoun. Currents through single glutamate receptor channels in outside-out patches from rat cerebellar granule cells. *J. Physiol. (Lond.)* **432**:143–202 (1991).
34. Howe, J. R., D. Colquhoun, and S. G. Cull-Candy. On the kinetics of large-conductance glutamate-receptor ion channels in rat cerebellar granule neurons. *Proc. R. Soc. Lond. B Biol. Sci.* **233**:407–422 (1988).
35. Wright, J. M., and L. M. Nowak. Voltage dependent change in probability of opening (nP_o) of *N*-methyl-D-aspartate (NMDA) channels in Mg free solutions. *Biophys. J.* **57**:127a (1990).
36. Patlak, J. B., K. A. F. Gration, and P. N. R. Usherwood. Single glutamate-activated channels in locust muscle. *Nature (Lond.)* **278**:643–645 (1979).
37. Perkins, M. N., T. W. Stone, J. F. Collins, and K. Curry. Phosphonate analogues of carboxylic acid antagonists on rat cortical neurons. *Neurosci. Lett.* **23**:333–336 (1981).
38. Nowak, L., P. Bregestovski, P. Ascher, A. Herbert, and A. Prochiantz. Magnesium gates glutamate-activated channels in mouse central neurones. *Nature (Lond.)* **307**:462–465 (1984).
39. Mayer, M., G. L. Westbrook, and P. B. Guthrie. Voltage-dependent block by Mg^{2+} of NMDA responses in spinal cord neurones. *Nature (Lond.)* **309**:261–263 (1984).
40. Huettner, J. E., and B. P. Bean. Block of *N*-methyl-D-aspartate activated current by the anti-convulsant MK-801: selective binding to open channels. *Proc. Natl. Acad. Sci. USA* **85**:1307–1311 (1988).
41. Cull-Candy, S. G., J. R. Howe, and D. C. Ogden. Noise and single channels activated by excitatory amino acids in rat cerebellar granule neurones. *J. Physiol. (Lond.)* **400**:189–222 (1988).
42. Honoré, T., S. N. Davies, J. Drejer, E. J. Fletcher, P. Jacobsen, D. Lodge, and F. E. Nielsen. Quinoxalidiones: potent competitive non-NMDA glutamate receptor antagonists. *Science* **241**:701–703 (1988).
43. Sucher, N. J., E. Aizemann, and S. A. Lipton. *N*-Methyl-D-aspartate antagonists prevent kainate neurotoxicity in rat retinal ganglion cells *in vitro*. *J. Neurosci.* **11**:966–971 (1991).
44. Drejer, J., and T. Honoré. New quinoxalinediones show potent antagonism of quisqualate response in cultured mouse cortical neurons. *Neurosci. Lett.* **87**:104–108 (1988).
45. Randle, J. C., T. Guet, C. Bobichon, C. Moreau, P. Curutchet, B. Lambolez, L. P. de Carvalho, A. Cordi, and J. M. Lepagnol. Quinoxaline derivatives: structure-activity relationships and physiological implications of inhibition of *N*-methyl-D-aspartate and non-*N*-methyl-D-aspartate receptor-mediated currents and synaptic potentials. *Mol. Pharmacol.* **41**:337–345 (1992).
46. Blake, J. F., M. W. Brown, and G. L. Collingridge. CNQX blocks acidic amino acid induced depolarizations and synaptic components mediated by non-NMDA receptors in rat hippocampal slices. *Neurosci. Lett.* **89**:182–186 (1988).
47. Frenguelli, B. G., J. F. Blake, M. W. Brown, and G. L. Collingridge. Electrogenic uptake contributes a major component of the depolarizing action of L-glutamate in rat hippocampal slices. *Br. J. Pharmacol.* **102**:355–362 (1991).
48. Jahr, C. E., and C. F. Stevens. Glutamate activates multiple single channel conductances in hippocampal neurons. *Nature (Lond.)* **325**:522–525 (1987).
49. Brackley, P. T. H., and P. N. R. Usherwood. Evidence for chimeric kainate/NMDA receptors expressed in *Xenopus* oocytes from mammalian and amphibian RNA. *J. Pharmacol. Exp. Ther.*, in press.
50. Samson, M. S. P., and P. N. R. Usherwood. Single-channel studies of glutamate receptors. *Int. Rev. Neurobiol.* **32**:51–106 (1990).
51. Zorumski, C. F., and L. L. Thio. Properties of vertebrate glutamate receptors: calcium mobilization and desensitization. *Prog. Neurobiol.* **39**:295–336 (1992).
52. Anholt, R., J. Lindstrom, and M. Montal. Stabilization of acetylcholine receptor channels by lipids in cholate solution and during reconstitution in vesicles. *J. Biol. Chem.* **256**:4377–4387 (1981).
53. Schurholz, T., J. Weber, and E. Neumann. Reconstitution of the *Torpedo californica* nicotinic acetylcholine receptor into planar lipid bilayers. *Bioelectrochem. Bioenerg.* **21**:71–81 (1989).
54. Schindler, H., F. Spilleke, and E. Neumann. Different channel properties of *Torpedo* acetylcholine receptor monomers and dimers reconstituted in planar membranes. *Proc. Natl. Acad. Sci. USA* **81**:6222–6226 (1984).
55. Geletyuk, V. I., and V. N. Kazachenko. Single Cl^- channels in molluscan neurones: multiplicity of the conductance states. *J. Membr. Biol.* **86**:9–15 (1985).
56. Krouse, M. E., G. T. Schneider, and P. W. Gage. A large anion-selective channel has seven conductance levels. *Nature (Lond.)* **319**:58–60 (1986).

Send reprint requests to: Peter N. R. Usherwood, Department of Life Science, University of Nottingham, Nottingham, NG7 2RD, UK.